

## ARTICLES

## Rotational Dynamics of Coumarin 153 in Supercritical Fluoroform

Noritsugu Kometani,\* Yuji Hoshihara, and Yoshiro Yonezawa

*Department of Applied Chemistry, Graduate School of Engineering, Osaka City University, Sugimoto 3-3-138, Sumiyoshi-ku, Osaka 558-8585, Japan*

Okitsugu Kajimoto

*Graduate School of Science, Kyoto University, Sakyo-ku, Kyoto 606-8502, Japan*

Kimihiko Hara

*Research Center for Low Temperature and Materials Sciences, Kyoto University, Sakyo-ku, Kyoto 606-8502, Japan*

Naoki Ito

*Department of Chemistry, The Pennsylvania State University, University Park, Pennsylvania 16802**Received: May 18, 2004; In Final Form: August 11, 2004*

Subpicosecond fluorescence anisotropy decay curves have been measured using the fluorescence up-conversion technique to examine the rotational dynamics of coumarin 153 (C153) in supercritical fluoroform ( $T = 302$  and  $310$  K). For reduced densities ( $\rho_r = \rho/\rho_c$ ) above 0.9, the rotation times of C153 increase with density. For reduced densities lower than 0.9, the rotation times increase with decreasing density and has a maximum at a density near  $\rho_r = 0.5$ . The comparison with the extrapolation of the data in polar aprotic solvents indicates that the local solvent density around the solute exceeds about 4 times the bulk density at a density near  $\rho_r = 0.5$ , which is consistent with those obtained from the steady-state electronic spectral shifts.

## Introduction

Supercritical fluids at temperatures slightly above their critical temperatures ( $T_c$ ) have unique properties distinct from conventional solvents. Among them, the continuous tunability of the solvent density from gaslike to liquidlike region with relatively modest pressure variation is of great interest from viewpoints of fundamental physical chemistry as well as practical applications because this accompanies the change in various solvent properties such as solubility, dielectric constant, viscosity, etc.<sup>1–3</sup>

Studies of solvation in supercritical fluids have revealed that the local solvent density around the solute is often higher than that of the bulk fluid due to the attractive solute–solvent interaction and the high compressibility of the fluid near the critical point.<sup>4,5</sup> It is thus interesting to examine how the solute dynamics is influenced by such unique solvation in supercritical fluids. The rotational dynamics has been intensively studied in liquid solutions for a long time and is suitable for this purpose.<sup>6</sup> There have been a lot of experimental studies on the rotational dynamics of the solvent molecule under the supercritical conditions using NMR spectroscopy,<sup>7–13</sup> light scattering spectroscopy,<sup>14–16</sup> far-IR absorption spectroscopy,<sup>17</sup> and optical Kerr effect measurement.<sup>18</sup> However, only a few works have been reported so far that have examined the solute rotational dynamics in supercritical fluids.

In the earliest work, Bright and co-workers<sup>19</sup> studied the rotational dynamics of 6-propionyl-2-(dimethylamino)naphthalene (PRODAN) in supercritical  $N_2O$  ( $T_r = T/T_c = 1.01$ ). They measured the rotation times of PRODAN in the density region higher than  $\rho_r = \rho/\rho_c = 1.0$  and found that the rotation times increased from  $\sim 10$  ps at high densities to  $\sim 40$  ps near the critical density. Similar results were observed for the rotation times of *N,N'*-bis(2,5-*tert*-butylphenyl)-3,4,9,10-perylenecarboxodiimide (BTBP) in different supercritical fluids (carbon dioxide and fluoroform).<sup>20</sup> deGrazia et al.<sup>21</sup> examined the rotational relaxation of copper 2,2,3-trimethyl-6,6,7,7,8,8,8-heptafluoro-3,5-octanedionate in supercritical carbon dioxide and reported the similar finding to those of Bright and co-workers.

Anderton and Kauffman<sup>22</sup> measured the rotation times of two solutes, *trans*-1,4-diphenylbutadiene (DPB) and *trans*-4-(hydroxymethyl)stilbene (HMS) in supercritical carbon dioxide ( $T_r = 1.01$ ). In contrast to the results of Bright and co-workers, they observed that the rotation times of both solutes increased with increasing density from  $\rho_r = \sim 0.65$  to 2.0. Heitz and Maroncelli<sup>23</sup> also reported the similar results for the rotation times of BTBP, 1,3,6,8-tetraphenylpyrene, and 9,10-bis(phenylethynyl)anthracene (PEA) in supercritical carbon dioxide ( $T_r = 1.01$ ). The rotation times of all solutes increased with increasing density, which was approximately consistent with simple hydrodynamic theories in the density region higher than

\* Corresponding author. E-mail: kometani@a-chem.eng.osaka-cu.ac.jp.

$\rho_r = 1$ . The rotation times of PEA were found to deviate from hydrodynamic predictions for densities near and below the critical density, which was attributed to the local solvent density augmentation around the solute.

In the present study, we have measured time-resolved fluorescence anisotropy of coumarin 153 (C153) in supercritical fluoroform at  $T = 302$  K ( $T_r = T/T_c \approx 1.01$ ) and  $T = 310$  K ( $T_r \approx 1.04$ ) using subpicosecond fluorescence up-conversion techniques to examine the rotational dynamics of the solute. C153 has been employed as a probe, as its steady-state spectral properties in several supercritical fluids as well as the rotation times in a variety of liquid solvents have already been studied in detail.<sup>24–27</sup> The density dependence of the rotation times has been examined over a wide range of reduced densities:  $\rho_r = 0.45–1.8$ . The results are discussed in comparison with those in polar aprotic liquid solutions reported by Horng et al.<sup>24</sup>

## Experimental Section

Laser grade C153 (Lamda Physik) was used as received. Fluoroform (Daikin Industries Ltd., 99.95% purity) was used without further purification. The concentrations of sample solutions were  $\sim 5 \times 10^{-5}$  M.

Time-resolved fluorescence anisotropies were measured using the fluorescence up-conversion technique. The setup of the up-conversion laser system has been already described elsewhere.<sup>26</sup> In brief, a 800 nm laser pulse (80 fs duration, 80 MHz repetition rate) was generated by a mode-locked Ti:sapphire laser (Spectra Physics, Tsunami model 3960) pumped by a Nd:YVO<sub>3</sub> diode laser (Millennia V). The second harmonic radiation ( $\lambda_{\text{ex}} = 400$  nm) was generated by a 1.5 mm LBO crystal and used as an excitation. To obtain the parallel and perpendicular polarized components of the sample fluorescence, the polarization of the excitation light was controlled with a Glan-laser prism and a half-wave plate placed in the front of the sample cell. The fluorescence was focused on a 0.5 mm BBO crystal with a lens. The residual fundamental beam was subject to a variable optical delay and focused on the same BBO crystal with a lens for up-converting the sample fluorescence. The up-converted light was filtered, monochromatized by a monochromator (Oriel, model 77200), and detected with a photomultiplier. The wavelength of the up-converted light was 305 nm, which corresponded to the fluorescence of about 500 nm. The overall instrumental response of the system is about 250 fs (fwhm), as estimated from the cross-correlation between the excitation and fundamental laser pulses.

The high-pressure optical cell was made of stainless steel and equipped with two fused quartz windows (4 mm in thickness). The optical path length is 2 mm. The sample solution was circulated within the cell with a small magnetic stirrer. The temperature was controlled by circulating thermostated water and monitored with a thermocouple inserted into the cell. Fluoroform was introduced into the cell with a HPLC pump (JASCO, SCF get), and pressure was monitored by a strain pressure gauge (Kyowa, PGM-500KD). It is noted that the pressure-induced polarization scrambling due to the fused quartz is negligible at the pressures studied here.<sup>28</sup>

## Results

Figure 1 shows the typical decay curves for the parallel- ( $I_{\parallel}$ ) and perpendicular-polarized ( $I_{\perp}$ ) components of the fluorescence of C153 in supercritical fluoroform at (a)  $T = 310$  K,  $P = 9.08$  MPa

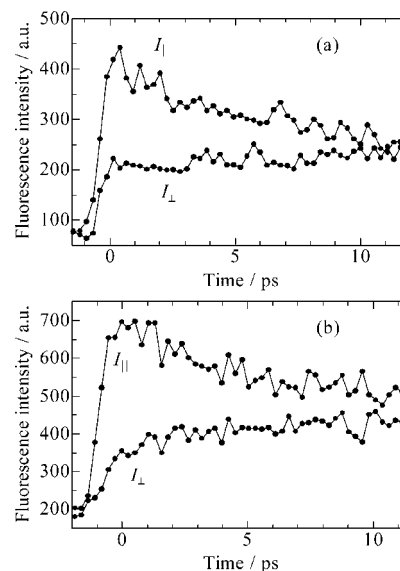


**Figure 1.** Decay curves for the parallel- ( $I_{\parallel}$ ) and perpendicular-polarized ( $I_{\perp}$ ) components of the fluorescence of C153 in supercritical fluoroform at (a)  $T = 310$  K,  $P = 9.08$  MPa and (b)  $T = 302$  K,  $P = 4.81$  MPa. The wavelength of the monitored fluorescence is 500 nm.

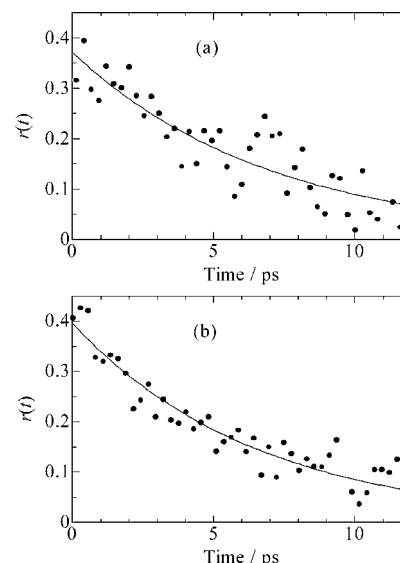


**Figure 2.** Fluorescence anisotropy decay curves of C153 in supercritical fluoroform at (a)  $T = 310$  K,  $P = 9.08$  MPa and (b)  $T = 302$  K,  $P = 4.81$  MPa. The solid lines represent the results of fits by eq 2. The wavelength of the monitored fluorescence is 500 nm.

MPa, and (b)  $T = 302$  K,  $P = 4.81$  MPa. The time-resolved fluorescence anisotropy  $r(t)$  was calculated by

$$r(t) = \frac{I_{\parallel}(t) - I_{\perp}(t)}{I_{\parallel}(t) + 2I_{\perp}(t) - 3b} \quad (1)$$

where  $I_{\parallel}(t)$  and  $I_{\perp}(t)$  denote the parallel- and perpendicular-polarized components of the fluorescence with respect to the polarization of the excitation light, and  $b$  is the background intensity determined by the signal level at  $t < 0$ . The magnitude of  $b$  was about 10–15% of the signal intensity. It is noted that  $r(t)$  was directly calculated from measured  $I_{\parallel}(t)$  and  $I_{\perp}(t)$  without deconvolution, since the instrumental response of the present system is much shorter than the time scale of rotation times observed here. The anisotropy decay curves  $r(t)$  corresponding to Figure 1 are illustrated in Figure 2. To obtain the rotation

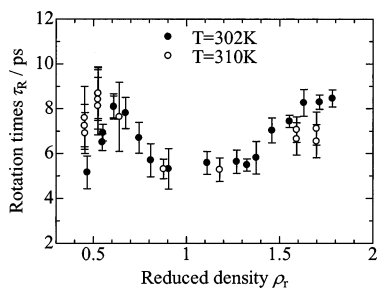


**Figure 3.** Rotation times of C153 in supercritical fluoroform as a function of reduced density. Filled and open circles denote the rotation times at  $T = 302$  and  $310$  K, respectively.

times  $\tau_R$  of C153, the  $r(t)$  data were fit to the single-exponential function

$$r(t) = r(0) \exp(-t/\tau_R) \quad (2)$$

in which  $r(0)$  and  $\tau_R$  were varied as parameters. The solid lines in Figure 2 represent the example of such fits. For all data sets, the single-exponential function was sufficient to reproduce the anisotropy decay curves within the  $S/N$  level of the data. It is found that the resulting  $r(0)$  values are  $0.36 \pm 0.03$  for all data sets, which is slightly lower than the theoretical limiting value for the parallel transition dipole between absorption and emission and agrees with the previous reports.<sup>24,26</sup>

Figure 3 summarizes the density dependence of the rotation times of C153 in supercritical fluoroform at  $T = 302$  and  $310$  K. The densities were calculated by the equation of state reported by Rubio and co-workers.<sup>29</sup> The rotation times at  $\rho_r = 0.55$  and  $0.61$  ( $T = 302$  K) and  $\rho_r = 0.45, 0.52, 1.59,$  and  $1.70$  ( $T = 310$  K) have been measured two or three times and are plotted together in Figure 3. It is found that the rotation times at both temperatures show the similar density dependence. For reduced densities above  $0.9$ , the rotation times at  $T = 302$  K decrease with decreasing density from  $8.5$  ps at  $\rho_r = 1.78$  to  $5.3$  ps at  $\rho_r = 0.9$ . The rotation times at  $T = 310$  K also decrease from  $7.1$  ps at  $\rho_r = 1.70$  to  $5.3$  ps at  $\rho_r = 0.9$ . This trend is somewhat similar to those observed by Anderton et al.<sup>22</sup> and Heitz et al.<sup>23</sup> More interesting behavior is found for reduced densities lower than  $0.9$ . The rotation times increase with decreasing density up to  $8.1$  ps at  $\rho_r = 0.61$  ( $T = 302$  K) and  $8.7$  ps at  $\rho_r = 0.53$  ( $T = 310$  K), and then begin to decrease with decreasing density.

## Discussion

The earliest theoretical approach to describe molecular rotational motion in liquid solutions is the Stokes–Einstein–Debye (SED) model, which is based on hydrodynamic theories.<sup>30,31</sup> The SED model assumes the structureless continuum solvent and the spherical shape of the solute. Perrin<sup>32</sup> and Kivelson et al.<sup>33</sup> have modified the SED model to take the effects of shape and size of both solute and solvent molecules into account. According to their theory, the rotation time  $\tau_R$  can be written by

$$\tau_R = \frac{V\eta}{k_B T} fC + \tau_0 \quad (3)$$

where  $V$  is the hydrodynamic volume of the rotating solute molecule,  $\eta$  is the solvent viscosity,  $k_B$  is the Boltzmann constant,  $f$  is a parameter which accounts for the shape of the solute,  $C$  is the boundary condition factor, and  $\tau_0$  is the inertial

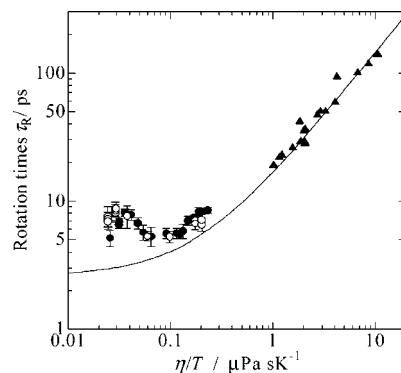


**Figure 4.** Rotation times of C153 as a function of  $\eta/T$ . Filled and open circles are the rotation times in supercritical fluoroform at  $T = 302$  and  $310$  K, respectively. Triangles are the literature data in polar aprotic liquid solvents at atmosphere pressure.<sup>12</sup> The solid line represents the linear regression (eq 3) to the rotation times in liquid solvents.

rotor time of the solute, respectively. The inertial rotor time  $\tau_0$  is given by<sup>34</sup>

$$\tau_0 = \frac{2\pi}{9} \sqrt{\frac{I}{k_B T}} \quad (4)$$

where  $I$  is the moment of inertia. According to semiempirical calculations,<sup>24</sup> the  $S_0$ – $S_1$  transition moment of C153 lies approximately parallel to the longest molecular axis. It is therefore not unreasonable to assume that the rotation about the axis perpendicular to the aromatic plane of C153 is effective for the fluorescence anisotropy decay. Under this assumption,  $I = 5.7 \times 10^{-47}$  kg·m<sup>2</sup> and  $\tau_0 = 2.6$  ps are calculated. It is noted that  $\tau_0$  estimated by eq 4 is not always consistent with observed  $\tau_0$ .<sup>35</sup> However, the choice of the  $\tau_0$  value has little influence on our final results of effective densities as described below.

It is noteworthy that eq 3 has been derived under the assumption that the rotational motion is completely diffusive. This assumption will break down in the case of the low-density gaseous region where the time between the binary collisions is comparable to the rotation time.<sup>36,37</sup> It is therefore important to discuss the applicable density region of eq 3 in the present system. Patel and co-worker have examined the rotational dynamics of HMS and DPB in supercritical CO<sub>2</sub> ( $T = 310$  K,  $\rho_r = 0.25$ – $2.0$ ) using computer simulations and compared them with the experimental results.<sup>38</sup> They observed that the rotation times of these solutes calculated using the diffusive-limit prediction were comparable to those experimentally observed down to  $\rho_r = 0.5$ , indicating that the solute rotational motion is essentially diffusive for densities higher than  $\rho_r = 0.5$ . We recently conducted the computer simulations of C153 in supercritical fluoroform ( $T = 310$  K,  $\rho_r = 0.25$ – $2.0$ ) and observed that the angler velocity autocorrelation functions of C153 decay more rapidly than the orientational correlation functions beyond  $\rho_r = 0.5$ .<sup>39</sup> Considering these observations, we have suggested that the rotational motion of C153 is diffusive and eq 3 may be applicable in the density region examined here.

As indicated by eq 3, the hydrodynamic model predicts the linear correlation between  $\tau_R$  and  $\eta/T$  when  $V$ ,  $C$ , and  $f$  are constant. Figure 4 shows the correlation between the rotation times of C153 in supercritical fluoroform and  $\eta/T$ . Viscosities of supercritical fluoroform were determined using the model equation and coefficients reported by Shan et al.<sup>40</sup> For comparison, the rotation times of C153 in polar aprotic solvents reported by Horng et al.<sup>24</sup> are also plotted in Figure 4. Horng et al. have observed that the rotational dynamics of C153 in

polar aprotic and hydrogen-bonding solvents behaved identically and behaved as much as would be expected from a purely hydrodynamic model. We have therefore fit eq 3 to the data in polar aprotic solvents with  $VfC/k_B$  varied and  $\tau_0 = 2.6$  ps fixed. The solid line in Figure 4 is the result of fits (fit parameter,  $VfC/k_B = 14.3 \mu\text{Pa}^{-1}\text{K}$ ), demonstrating the good agreement between the experiment and theory as mentioned above.

We now compare the rotation times of C153 in supercritical fluoroform with those extrapolated from the data in liquid solvents by the modified SED model (solid line in Figure 4). In the high viscosity region, the behavior of the density dependence of the rotation times in supercritical fluoroform is similar to that of the model predictions, although they are 30–50% larger than the predictions. This observations are consistent with those obtained by Anderton et al. as well as Heitz et al.<sup>22,23</sup> However, the rotation times at medium and low viscosities are at most ~400% larger than the model predictions, and the behavior of the density dependence is completely different. Biswas and co-workers<sup>27</sup> measured the density dependence of steady-state excitation and emission spectra of C153 in supercritical fluoroform ( $T = 304.3$  K). They found that the local solvent density exceeds about 4 times the bulk density and the density augmentation was maximized near  $\rho_r = 0.5$ . It is therefore reasonable to ascribe the difference between the observed rotation times and model predictions to the influence of the local density augmentation. The local density can be estimated from the rotation times in the same manner as reported by Heitz et al.<sup>23</sup> The effective local density,  $\rho_{\text{eff}}$ , is defined by

$$\tau_R^{\text{obs}}(\rho) = A \frac{\eta(\rho_{\text{eff}})}{T} + \tau_0 \quad (5)$$

where  $\tau_R^{\text{obs}}(\rho)$  is the observed rotation time at given density and  $A$  is a constant. The values  $A = 14.3 \mu\text{Pa}^{-1}\text{K}$  and  $\tau_0 = 2.6$  ps, determined by fitting to the data in polar aprotic solvents, are used. As aforementioned, 1 ps (~40%) increase or decrease in  $\tau_0$  results in only 10% variation in  $\rho_{\text{eff}}$  and no impact on the general trend of the density dependence. For this reason, the choice of the  $\tau_0$  value is not so crucial for the following discussions in this study.

The relative local density,  $\rho_{\text{eff}}/\rho$ , and the local density augmentation factor,  $(\rho_{\text{eff}} - \rho)/\rho_c$ , at  $T = 302$  and 310 K obtained in this manner are shown in Figure 5. It is found for both temperatures that the local density augmentation is not so remarkable for densities higher than  $\rho_r = 1$ . However, for densities lower than  $\rho_r = 1$ , both the local density augmentation factor and relative local density increase with decreasing density and the local density augmentation factor has a maximum at a density near  $\rho_r = 0.5$ . At this density,  $(\rho_{\text{eff}} - \rho)/\rho_c$  amounts to about 1.5 and the local density exceeds about 4 times the bulk density. These observations are surprisingly in good agreement with those obtained from the steady-state spectral shifts within the uncertainties of the data,<sup>27</sup> although the magnitude of  $(\rho_{\text{eff}} - \rho)/\rho_c$  deduced from the spectral shifts is about 30% smaller than that of this work. The similar observation was reported for PEA in supercritical carbon dioxide for reduced densities between 0.8 and 1.9.<sup>23</sup> There is no obvious reason that the effective densities obtained from the rotation times and the spectral shifts should be identical. However, this behavior is not unexpected when considering the following facts. The length scale of the friction sensed by the rotational motion of the solute is expected to be the order of molecular size, since it mainly arises from collisions between solute and solvent molecules. On the other hand, according to the recent studies by computer simulations,<sup>38,41</sup> the local density estimated from the spectral

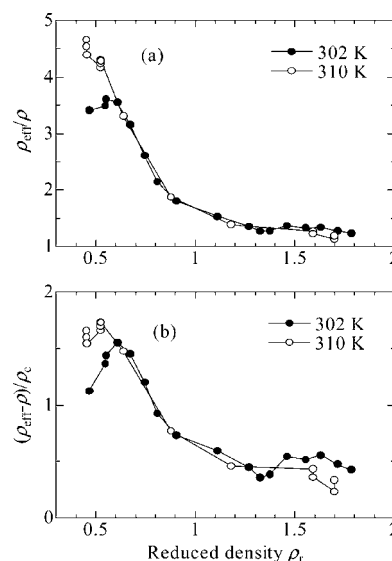


**Figure 5.** Effective densities determined from the rotation times as described in the text. The values of (a)  $\rho_{\text{eff}}/\rho$  and (b)  $(\rho_{\text{eff}} - \rho)/\rho_c$  are plotted as a function of reduced density. Filled and open circles represent the data at  $T = 302$  and 310 K, respectively.

shifts is closely parallel to that obtained from the solvent density within the first solvation shell, implying that the length scale of the local density probed by the spectral shifts is also the order of molecular size. The similarity in the local densities observed here may support this fact that the length scale of the rotational friction is nearly the same as that probed by the spectral shifts of the solute.

## Conclusions

The present study has demonstrated how the rotational dynamics of C153 in supercritical fluoroform is influenced by the local density augmentation around the solute for densities of  $\rho_r = 0.45$ –1.8 at two temperatures,  $T = 302$  and 310 K. The magnitude of the local density augmentation estimated from the rotation times is in good agreement with those deduced from the steady-state spectral shifts, implying that the length scale of the friction sensed by the rotation of C153 is almost the same as that on which the spectral shifts are influenced by the surrounding solvent.

## References and Notes

- (1) The special issue of *Chem. Rev.* (1999, 99 (2)) edited by R. Noyori provides useful introductions to the recent work in this area.
- (2) *Supercritical Fluid Engineering Science—Fundamentals and Applications*; Kiran, E., Brennecke, J. F., Eds.; ACS Symposium Series 514; American Chemical Society: Washington, DC, 1993.
- (3) *Applications of Supercritical Fluids in Industrial Analysis*; Dean, J. R., Ed.; CRC Press: Boca Raton, FL, 1993.
- (4) Kajimoto, O. *Chem. Rev.* 1999, 99, 355.
- (5) Tucker, S. C. *Chem. Rev.* 1999, 99, 391.
- (6) See for example: *Rotational Dynamics of Small and Macromolecules*, 4th ed.; Dorfmueller, T., Pecora, R., Eds.; Springer-Verlag: Berlin, 1987.
- (7) Jonas, J.; DeFries, T.; Lamb, W. J. *J. Chem. Phys.* 1978, 68, 2988.
- (8) Lamb, W. J.; Jonas, J. *J. Chem. Phys.* 1981, 74, 913.
- (9) Zerda, T. W.; Schroeder, J.; Jonas, J. *J. Chem. Phys.* 1981, 75, 1612.
- (10) Tsukahara, T.; Harada, M.; Ikeda, Y.; Tomiyasu, H. *Chem. Lett.* 2000, 4, 420.
- (11) Tsukahara, T.; Harada, M.; Tomiyasu, H.; Ikeda, Y. *J. Supercrit. Fluids* 2003, 26, 73.
- (12) Matubayasi, N.; Nakao, N.; Nakahara, M. *J. Chem. Phys.* 2001, 114, 4107.
- (13) Umecky, T.; Kanakubo, M.; Ikushima, Y. *J. Phys. Chem. B* 2003, 107, 12003.



- (14) Baglin, F. G.; Versmold, H.; Zimmermann, U. *Mol. Phys.* **1984**, *53*, 1225.
- (15) Okazaki, A.; Matsumoto, M.; Okada, I.; Maeda, K.; Kataoka, Y. *J. Chem. Phys.* **1995**, *103*, 8594.
- (16) Okazaki, S.; Terauchi, N.; Okada, I. *J. Mol. Liq.* **1995**, *65/66*, 309.
- (17) Saitow, K.; Ohtake, H.; Sarukura, N.; Nishikawa, K. *Chem. Phys. Lett.* **2001**, *341*, 86.
- (18) Kiyohara, K.; Kimura, Y.; Takebayashi, Y.; Hirota, N.; Ohta, K. *J. Chem. Phys.* **2002**, *117*, 9867.
- (19) Betts, T. A.; Zagrobelny, J.; Bright, F. V. *J. Am. Chem. Soc.* **1992**, *114*, 8163.
- (20) Heitz, M. P.; Bright, F. V. *J. Phys. Chem.* **1996**, *100*, 6889.
- (21) deGrazia, J. L.; Randolph, T. W.; O'Brien, J. A. *J. Phys. Chem. A* **1998**, *102*, 1674.
- (22) Anderton, R. M.; Kauffman, J. F. *J. Phys. Chem.* **1995**, *99*, 13759.
- (23) Heitz, M. P.; Maroncelli, M. *J. Phys. Chem. A* **1997**, *101*, 5852.
- (24) Horng, M.-L.; Gardecki, J. A.; Maroncelli, M. *J. Phys. Chem. A* **1997**, *101*, 1030.
- (25) Kimura, Y.; Hirota, N. *J. Chem. Phys.* **1999**, *111*, 5474.
- (26) Ito, N.; Kajimoto, O.; Hara, K. *J. Phys. Chem. A* **2002**, *106*, 6024.
- (27) Biswas, R.; Lewis, J. E.; Maroncelli, M. *Chem. Phys. Lett.* **1999**, *310*, 485.
- (28) Chryssomallis, G. S.; Drickamer, H. G.; Weber, G. *J. Appl. Phys.* **1978**, *49*, 3084.
- (29) Rubio, R. G.; Zollweg, J. A.; Streett, W. B. *Ber. Bunsen-Ges. Phys. Chem.* **1989**, *93*, 791.
- (30) Einstein, A. *Ann. Phys. (Leipzig)* **1906**, *19*, 371.
- (31) Debye, P. *Polar Molecules*; Dover: New York, 1929.
- (32) Perrin, F. *J. Phys. Radium* **1934**, *5*, 497.
- (33) Kivelson, D.; Kivelson, M. G.; Oppenheim, I. *J. Chem. Phys.* **1970**, *52*, 1810. Kivelson, D. *Discuss. Faraday Soc.* **1977**, *11*, 7. Dote, J. L.; Kivelson, D.; Schwartz, R. N. *J. Phys. Chem.* **1981**, *85*, 2169.
- (34) Bartoli, F. J.; Litovitz, T. A. *J. Chem. Phys.* **1972**, *56*, 404. Bartoli, F. J.; Litovitz, T. A. *J. Chem. Phys.* **1972**, *56*, 413.
- (35) Zhang, Y.; Sluch, M. I.; Somoza, M. M.; Berg, M. A. *J. Chem. Phys.* **2001**, *115*, 4212.
- (36) Gordon, R. G. *J. Chem. Phys.* **1965**, *43*, 1307. Gordon, R. G. *J. Chem. Phys.* **1966**, *44*, 1830.
- (37) Baskin, J. S.; Gupta, M.; Chachivilis, M.; Zewail, A. H. *Chem. Phys. Lett.* **1997**, *275*, 437. Baskin, J. S.; Chachivilis, M.; Gupta, M.; Zewail, A. H. *J. Phys. Chem. A* **1998**, *102*, 4158.
- (38) Patel, N.; Biswas, R.; Maroncelli, M. *J. Phys. Chem. B* **2002**, *106*, 7096.
- (39) Kometani, N.; Maroncelli, M. Manuscript in preparation.
- (40) Shan, Z.; Penoncello, S.; Jacobsen, R. *ASHRAE Trans.* **2000**, *106*, 757.
- (41) Song, W.; Biswas, R.; Maroncelli, M. *J. Phys. Chem. A* **2000**, *104*, 6924.